Доклади на Българската академия на науките
Comptes rendus de l'Académie bulgare des Sciences
Tome 66, No 6, 2013

MATHEMATIQUES
Mathématiques appliquées

DYNAMIC BEHAVIOUR OF PIEZOELECTRIC SOLID VIA CNN APPROACH

Tsviatko Rangelov, Angela Slavova

(*Submitted by Academician Bl. Sendov on January 25, 2013*)

Abstract

Considered is piezoelectric solid under anti–plane mechanical and in–plane electrical load. Dynamic behaviour of the corresponding initial–boundary value problem is studied by means of Cellular Neural Networks (CNN) approach. RTD-based CNN model is constructed and simulations of this model are presented. By applying Lyapunov majorizing equations technique the dynamics of the proposed problem is investigated.

Key words: piezoelectric finite solid, Cellular Neural Network, RTD-based CNN, Lyapunov majorizing equations

2000 Mathematics Subject Classification: 74F15, 92B20, 35K57, 35Q68

1. Introduction. Piezoelectric materials (PEM) have wide applications in the recent years in smart intelligent systems. Mathematical modelling of PEM leads to complicated initial–boundary value problems (IBVP) for coupled system of partial differential equations of second order, see [7].

The aim of the work is to study the behaviour of the solutions of IBVP by means of resonant tunnel diode (RTD) based Cellular Neural Networks (CNN) approach [2, 3, 9]. The study is motivated by recent work [5] in which it is reported that RTD, a class of quantum effect devices, is an excellent candidate for both analogue and digital applications because of their structural simplicity, relative ease of fabrication, inherent speed and design flexibility. Many methods used in pattern recognition can be easily implemented by the RTD-based CNN approach.

The authors acknowledge the support of the Bulgarian National Science Fund under Grant No. DID 02/15.

2. RTD-based CNN and statement of the problem. CNN is simply an analogue dynamic processor array, made of cells, which contain linear capacitors, linear resistors, linear and nonlinear controlled sources [2, 3]. Let us consider a two-dimensional grid with 3×3 neighbourhood system. One of the key features of CNN is that the individual cells are nonlinear dynamical systems, but the coupling between them is linear. Roughly speaking, one could say that these arrays are nonlinear but have a linear spatial structure, which makes the use of techniques for their investigation common in engineering or physics attractive.

We will give general definition of a CNN which follows the original one [2]:

Definition 1. *An $M \times M$ cellular neural network is defined mathematically by four specifications*:

1) *CNN cell dynamics*;

2) *CNN synaptic law which represents the interactions* (*spatial coupling*) *within the neighbour cells*;

3) *Boundary conditions*;

4) *Initial conditions.*

In terms of the definition we can present the dynamical systems describing CNN. For general CNN whose cells are made of time-invariant circuit elements, each cell $C(ij)$ is characterized by its CNN cell dynamics

$$\dot{x}_{ij} = -g(x_{ij}, u_{ij}, I^s_{ij}), \tag{1}$$

where $x_{ij} \in \mathbf{R}^m$, u_{ij} is usually a scalar. In most cases, the interactions (spatial coupling) with the neighbour cell $C(i+k, j+l)$ are specified by a CNN synaptic law

$$\begin{aligned} I^s_{ij} &= A_{ij,kl} x_{i+k,j+l} \\ &+ \tilde{A}_{ij,kl} * f_{kl}(x_{ij}, x_{i+k,j+l}) \\ &+ \tilde{B}_{ij,kl} * u_{i+k,j+l}(t). \end{aligned} \tag{2}$$

The first term $A_{ij,kl} x_{i+k,j+l}$ of (2) is simply a linear feedback of the states of the neighbourhood nodes. The second term provides an arbitrary nonlinear coupling, and the third term accounts for the contributions from the external inputs of each neighbour cell that is located in the N_r neighbourhood.

One-dimensional original RTD-based CNN without input and threshold terms is defined as follows [5, 6]:

$$\frac{dx_j}{dt} = -f(x_j(t)) + \alpha x_j(t) + \gamma x_{j-1}(t) + \delta x_{j+1}(t),$$

where the real parameters α, γ, δ with $\gamma \geq 0$, $\delta \geq 0$, and $\gamma + \delta \neq 0$ constitute the so-called space-invariant template that measures the synaptic weights of self-feedback and neighbourhood interaction.

It is known that some autonomous CNN represent an excellent approximation to nonlinear partial differential equations (PDEs) [8, 9]. The intrinsic space distributed topology makes the CNN able to produce real-time solutions of nonlinear PDEs. Consider the following well-known PDE, generally referred to in the literature as a reaction-diffusion equation:

$$\frac{\partial u}{\partial t} = f(u) + D\Delta u,$$

where $u \in \mathbf{R}^N$, $f \in \mathbf{R}^N$, D is a matrix with the diffusion coefficients, and Δ is Laplace operator in $\mathbf{R}^2$. There are several ways to approximate Laplace operator in discrete space by a CNN synaptic law with an appropriate A-template.

Following the approach of RTD-based CNN we shall study the IBVP for PEM solid under anti-plane mechanical and in-plane electrical load. Consider a finite transversally isotropic piezoelectric solid $\Omega \in \mathbf{R}^3$ with boundary S and poled in Ox_3 direction of a Cartesian coordinate system Ox in $\mathbf{R}^3$. Assume that Ω is subjected to anti-plane mechanical and in-plane electrical time-harmonic load. The only non-vanishing displacements are the anti-plane mechanical displacement $u_3(x,t)$ and in-plane electrical displacement $D_i(x,t)$, $i = 1,2$, $x = (x_1, x_2)$. We assume quasi-static approximation of piezoelectricity. Then the field equation of body forces and electric charges is given by balance equations

$$\frac{\partial \sigma_{i3}}{\partial x_i} = \rho \frac{\partial^2 u_3}{\partial t^2}, \quad \frac{\partial D_i}{\partial x_i} = 0, \tag{3}$$

in which the summation convention over repeated indices is applied. The relations: strain-displacement and electric field-potential are the following:

$$s_{i3} = \frac{\partial u_3}{\partial x_i}, \; E_i = -\frac{\partial \Phi}{\partial x_i}, \tag{4}$$

where σ_{i3}, s_{i3}, E_i, Φ, $\rho > 0$ are the stress tensor, strain tensor, electric field vector, electric potential and mass density respectively. The constitutive relations [6] are

$$\begin{aligned} \sigma_{i3} &= c_{44} s_{i3} - e_{15} E_i, \\ D_i &= e_{15} s_{i3} + \varepsilon E_i. \end{aligned} \tag{5}$$

After substituting (5) and (4) into (3), we obtain the following coupled system:

$$\begin{aligned} c_{44}\Delta u_3 \; + \; e_{15}\Delta\Phi &= \rho \frac{\partial^2 u_3}{\partial t^2}, \\ e_{15}\Delta u_3 \; - \; \varepsilon_{11}\Delta\Phi &= 0, \end{aligned} \tag{6}$$

where $c_{44} > 0$, $e_{15}, \varepsilon_{11} > 0$ are the shear stiffness, piezoelectric and dielectric permittivity constants, respectively. The boundary conditions on the boundary

$S \times (0,T)$ are given as a prescribed $\bar{u}_3, \bar{\Phi} \in H^1(S \times (0,T)$. Initial conditions are $u_3(x,0) = u_{30} \in H^1(\Omega)$, $\dfrac{\partial u_3}{\partial t}(x,0) = u_{31} \in L^2(\Omega)$. Following [1] the above IBVP for (6) admits unique solution $u_3, \Phi \in L^\infty(0,T;H^1(\Omega))$.

RTD-based CNN model of the coupled system (6) consisting of $n = MN$ cells is

$$
\begin{aligned}
(7)\ & c_{44}(u_{3,j-1} - 2u_{3,j} + u_{3,j+1}) + e_{15}(\Phi_{j-1} - 2\Phi_j + \Phi_{j+1}) - \rho\frac{d^2u_{3,j}}{dt^2} = 0,\\
& e_{15}(u_{3,j-1} - 2u_{3,j} + u_{3,j+1}) - \varepsilon_{11}(\Phi_{j-1} - 2\Phi_j + \Phi_{j+1}) = 0, 1 \le j \le n.
\end{aligned}
$$

Let use rewrite system (7) in the following way:

$$
\begin{aligned}
(8)\qquad & c_{44}A_1 * u_{3,j} + e_{15}A_1 * \Phi_j - \rho\frac{d^2u_{3,j}}{dt^2} = 0,\\
& e_{15}A_1 * u_{3,j} - \varepsilon_{11}A_1 * \Phi_j = 0, 1 \le j \le n,
\end{aligned}
$$

where A_1 is one-dimensional discretized Laplacian template $A_1 = (1,-2,1)$, $*$ is convolution operator defined below.

Definition 2. *For any cloning template A which defines the dynamic rule of the cell circuit, we define the convolution operator $*$ by the formula*

$$A * z_{ij} = \sum_{C(k,l)\in N_r(i,j)} A(k-i, l-j)z_{kl},$$

where $A(m,n)$ denotes the entry in the p-th row and r-th column of the cloning template, $p = -1,0,1$, and $r = -1,0,1$, respectively.

After expressing Φ_j from the second equation and substituting it in the first one, we obtain

$$(9)\qquad -\rho\frac{d^2u_{3,j}}{dt^2} + \left(c_{44} + \frac{e_{15}^2}{\varepsilon_{11}}\right)A_1 * u_{3,j} = 0.$$

For the sake of simplicity, the output of our RTD-based CNN model is a piecewise linear function $y(u_{3,j})$ given by

$$(10)\quad y(u_{3,j}) = au_{3,j} + b(|u_{3,j} - V_p| - |u_{3,j} - V_v|) - b(|u_{3,j} + V_p| - |u_{3,j} + V_v|),$$

where $a > 0$, $b < 0$ are constants, V_p, V_v $(0 < V_p < V_v)$ are the peak and valley voltage of the RTD (for the positive region of $u_{3,j}$), respectively. I_p and I_v are the peak and valley current, respectively. Notice that the output function is symmetric with respect to the origin (see Fig. 1).

We take fixed boundary conditions

$$u_{3,j}^0 = P_1, \quad u_{3,j}^{n+1} = P_2.$$

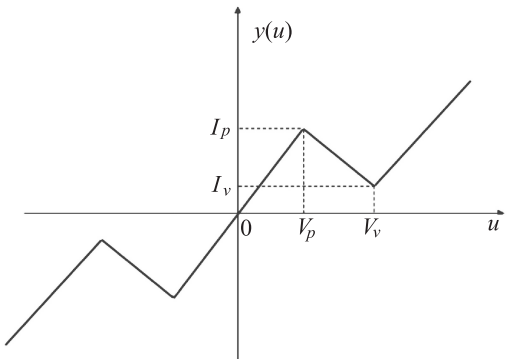

Fig. 1. The v-i characteristic of the output (10) of RTD-based CNN

Here CNN is simply clamped at its ends to some fixed potentials P_1, P_2. $u^0_{3,j}$ are the left-most nodes, $u^{n+1}_{3,j}$ are the right-most nodes. Initial conditions are $u_{3,j}(0) = u_0$.

In all simulations material constants of PZT4 are used: $c_{44} = 2.56 \times 10^{10}$ N/m^2, $e_{15} = 12.7$ C/m^2, $\varepsilon_{11} = 64.6 \times 10^{-10}$ C/Vm and $\rho = 7.5 \times 10^3$ kg/m^3.

After the simulation for the above RTD-based CNN model we obtain the numerical results for the solutions of the RTD-based CNN model (9) in Fig. 2. We consider 10×10 RTD-based CNN on 2-dimensional grid with axes i, j and $u_{3,j}$. Simulations are made for the different values of A_1-template.

Remark 1. In [6] it is pointed out that the bistable RTD-based CNN exhibits good performance for a number of interesting applications because of its high-speed processing and high cell density. Thus, it is possible that a new generation of lower-power, high-speed, and large array-size CNN appears with the introduction of the RTD-based CNN.

3. Dynamical behaviour of the RTD-based CNN model. For the analysis of dynamic behaviour of our RTD-based CNN model (9), we will apply the method of Lyapunov's finite majorizing equations [4]. Let us rewrite equation (9) in the following form:

$$\begin{aligned} \frac{dv_j}{dt} &= \frac{1}{\rho}\left(c_{44} + \frac{e_{15}^2}{\varepsilon_{11}}\right) A_1 * u_{3,j}, \\ \frac{du_{3,j}}{dt} &= v_j, 1 \le j \le n. \end{aligned} \tag{11}$$

The vector form of (11) is

$$\begin{aligned} \frac{dV}{dt} &= \frac{1}{\rho}\left(c_{44} + \frac{e_{15}^2}{\varepsilon_{11}}\right) U = F_1(U), \\ \frac{dU}{dt} &= V = F_2(V), \end{aligned} \tag{12}$$

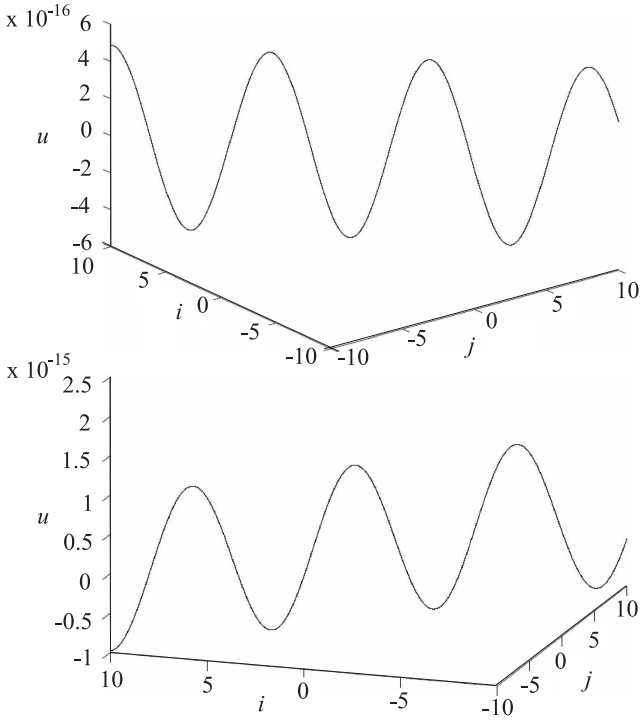

Fig. 2. Simulations of RTD-based CNN model (9)

where the cell state vector $(U, V) \in R^N$, i.e. it is produced by lining up every layer of the cell states in sequence. Let us introduce the following auxiliary system for (12):

$$\begin{aligned} \frac{dv}{dt} &= \chi(U,t), \\ \frac{du}{dt} &= \psi(V,t). \end{aligned} \tag{13}$$

The above system is a system of first order differential equations, hence we can write its equivalent integral system. Then in accordance with the method of Lyapunov majorizing equations [4], the following operator system can be written:

$$V(t) = L_1\chi(U,t),$$

$$U(t) = L_2\psi(V,t), t \in [0,T].$$

Operators L_1 and L_2 are linear and bounded and hence there exist constants ρ_1 and ρ_2 positive and such that the following inequality is satisfied:

$$\|L_1V(t)\| \leq \rho_1\|\chi(U,t)\|,$$

$$\|L_2U(t)\| \leq \rho_2\|\psi(V,t)\|.$$

If we go back to system (11) the following operator system can be written:

$$
\begin{aligned}
V(t) &= L_1\left[-\frac{1}{\rho}\left(c_{44}+\frac{e_{15}^2}{\varepsilon_{11}}\right)A_1U(t)\right], \\
U(t) &= L_2[V(t)].
\end{aligned} \tag{14}
$$

Now we construct the following system of Lyapunov's majorizing equations in the certain domain $U \in [0, u_*]$, $V \in [0, v_*]$:

$$
\begin{aligned}
\alpha(V) &= \rho_1\chi(U(\alpha)), \\
\beta(U) &= \rho_2\psi(V(\beta)),
\end{aligned} \tag{15}
$$

where $\alpha \geq |V|, \beta \geq |U|$.

Therefore, according to the properties of Lyapunov's majorizing equations [4], the following theorem has been proved:

Theorem 1. *Suppose that system* (15) *in the domains* $t \in [0, T]$ *and* $U \in [0, u_*]$, $V \in [0, v*]$ *has positive solutions* $\alpha = \alpha(v)$, $\beta = \beta(u)$ *for* $0 \leq U \leq u_*$, $0 \leq V \leq v_*$ *and* $||\alpha(v_*)|| \leq const.$, $\beta(u_*) \leq const.$ *Then system* (11) *has for* $U \in [0, u_*]$, $V \in [0, v_*]$ *solutions* $u_{3,j}(t)$, $v_j(t)$, *which are unique in the classes of functions* $C[t]$, $C[u]$ *and* $C[v]$. *These solutions can be found by the following convergent simple iterations*:

$$
\begin{aligned}
v_j^s &= L_1\left[\frac{1}{\rho}\left(c_{44}+\frac{e_{15}^2}{\varepsilon_{11}}\right)A_1 * u_{3,j}^{s-1}(t)\right], \\
u_{3,j}^s &= L_2 v_j^{s-1},\ 1 \leq j \leq n, \\
v_j^0 &\equiv v_j(0), \\
u_{3,j}^0 &\equiv u_{3,j}(0).
\end{aligned} \tag{16}
$$

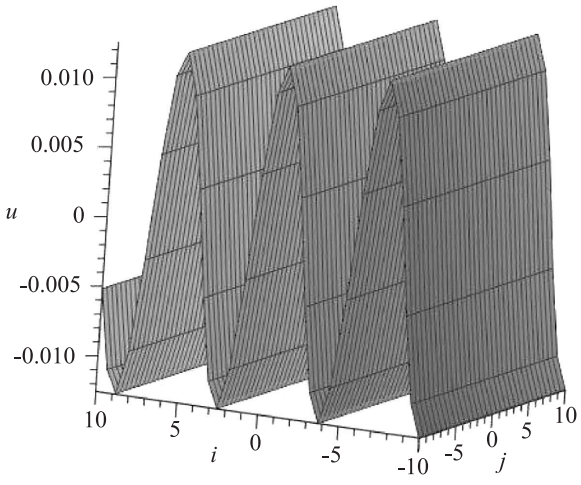

Fig. 3. Simulation of the solutions (16)

Remark 2. Let us consider iterations (16) and let us fix $t = \tau$, $0 \leq \tau \leq t$, $U = u_*$, $V = v_*$, $u_*, v_* \in [-1, 1]$. Then we can obtain the dynamic rules of our CNN model (9) and this system can be used as a dynamic transform of an initial state at any time.

After simulating the solutions (16), we obtain the following results.

Again we consider 10×10 RTD-based CNN on 2-dimensional grid with axes i, j and $u_{3,j}$. We see that for $u_{3,j} \in [-1, 1]$ the simulations based on the iterations (16) are similar to the simulations given in Fig. 2.

Remark 3. Many methods used in image processing and pattern recognition can be easily implemented by the RTD-based CNN approach, however, the mathematical analysis of the pattern formation, spatial chaos properties, and its dynamical behaviour are still not fully documented [5, 6]. In [6] the authors apply monotone iteration techniques with the concept upper and lower solutions to obtain travelling wave solutions for the various parameters given.

REFERENCES

[1] Akamatsu M., G. Nakamura. Appl. Anal., **81**, 2002, 129–141.

[2] Chua L. O., L. Yang. IEEE Trans. CAS, **35**, 1988, 1257–1290.

[3] Chua L. O., M. Hasler, G. S. Moschytz, J. Neirynsk. IEEE Trans. CAS-I, **42**, 1995, 559–557.

[4] Grebenikov E. A., Y. A. Ryabov. Constructive Methods in the Analysis of Nonlinear Systems. Mir Publisher, Moscow, 1979.

[5] Julián P., L. O. Chua. Int. J. Bifurcat. Chaos., **11**, 2000, 2913–2959.

[6] Hsu C. H., S. Y. Yang. J. Diff. Eq., **204**, 2004, 339–379.

[7] Parton V. Z., B. A. Kudryavtsev. Electromagnetoelasticity, Gordon and Breach Sci. Publ., New York, 1988.

[8] Roska T., L. O. Chua, D. Wolf, T. Kozek, R. Tetzlaff, F. Puffer. IEEE Trans. CAS-I, **42**, 1995, 807–815.

[9] Slavova A. Cellular Neural Networks: Dynamics and Modelling. Kluwer Academic Publishers, 2003.

Institute of Mathematics and Informatics
Bulgarian Academy of Sciences
Acad. G. Bonchev Str., Bl. 8
1113 Sofia, Bulgaria
e-mail: rangelov@math.bas.bg
slavova@math.bas.bg